Asynchronous transmitter release: control of exocytosis and endocytosis at the salamander rod synapse

F. Rieke and E. A. Schwartz*

Department of Pharmacological and Physiological Sciences, The University of Chicago, 947 East 58th Street, Chicago, IL 60637, USA

1. We have studied exocytosis and endocytosis in the synaptic terminal of salamander rods using a combination of Ca^{2+} imaging, capacitance measurement and the photolysis of Ca^{2+} buffers.

2. The average cytoplasmic Ca^{2+} concentration at the dark resting potential was 2–4 μM.

3. An average cytoplasmic Ca^{2+} concentration of 2–4 μM maintained a high rate of continuous exocytosis and endocytosis.

4. Changes in the rate of exocytosis were followed in less than 0·7 s by compensatory changes in the rate of endocytosis.

5. Vesicle cycling in the rod synapse is specialized for graded transmission and differs from that previously described for synapses that release synchronized bursts of transmitter.

Vertebrate photoreceptors continuously release transmitter in the dark and slow or stop the release when hyperpolarized by light (Trifonov, 1968). The absorption of a single photon hyperpolarizes a rod photoreceptor approximately 100 μV for 1 s (Schwartz, 1976; Capovilla, Hare & Owen, 1987), a voltage that is roughly 1000 times smaller and slower than the presynaptic polarization in the synaptic terminal of a spiking cell. Nonetheless, the response produced by the absorption of a single photon is reliably transmitted (Hecht, Shlaer & Pirenne, 1942), indicating that the rod synapse accurately transmits small changes in presynaptic voltage. We now report that vesicle cycling in the synaptic terminal of salamander rods is optimized for graded transmission and differs from that previously reported for synapses which signal the arrival of action potentials (see review by Augustine, Charlton & Smith, 1987).

A preliminary report of our findings has been presented at the 39th annual meeting of the Biophysical Society (Rieke & Schwartz, 1995).

METHODS

Salamanders (*Ambystoma tigrinum*) were decapitated and pithed following guidelines of the University of Chicago Institutional Animal Care and Use Committee. Rod photoreceptor inner segments with an attached synaptic terminal were isolated as described previously (Rieke & Schwartz, 1994). Membrane potential was controlled by a voltage clamp (List EPC7; Adams & List, Germany) in either whole-cell tight-seal or perforated-patch configurations. The pipette solution for whole-cell tight-seal recording contained (mM): caesium aspartate, 85; CsCl, 20; Hepes, 20; Mg-ATP, 1; Na-GTP, 0·1; leupeptin, 0·1; fluo-3, 0·1; pH 7·2. DM-nitrophen, nitr-5, diazo-2, $CaCl_2$ and Ca^{2+} buffers were added as indicated in the figure legends and text. Perforated-patch recordings were made after rods were incubated for 30 min at 4–6 °C in 2 μM fluo-3 AM (the acetoxymethyl ester form of fluo-3). The pipette solution for perforated-patch recording contained (mM): potassium aspartate, 75; NaCl, 20; K_2EGTA, 10; $CaCl_2$, 1; Hepes, 10; amphotericin B, 0·1; pH 7·2. The tip of the pipette was filled initially with amphotericin-free solution. The extracellular saline contained (mM): NaCl, 100; KCl, 2·5; $CaCl_2$, 1·2; $MgSO_4$, 1; sodium pyruvate, 1; NaH_2PO_4, 1; glucose, 8; Hepes, 10; the pH was adjusted to 7·4 with NaOH and the saline was supplemented with amino acids and vitamins formulated for Eagle's minimum essential medium (Cat. Nos. 320-1130 and 320-1120, respectively; Gibco). The extracellular saline was modified to suppress Ca^{2+}-activated Cl^- and K^+ currents during capacitance measurements by the addition of 0·4 mM niflumic acid and the replacement of K^+ with Cs^+. Access resistance was usually 6–10 MΩ in both configurations. In a series of twenty-four cells, the cell resistance was 1·2 $\pm$ 0·5 GΩ and the capacitance was 17 $\pm$ 5 pF (means $\pm$ S.D.).

Changes in capacitance were measured with a digital, phase-sensitive detector (see Joshi & Fernandez, 1988) as described previously (Rieke & Schwartz, 1994). Thirty-two cycles of a 20 mV peak-to-peak, 800 Hz sinusoidal voltage were added to a holding potential of −60 mV. Thus, the membrane potential remained 5–10 mV below the activation range of the voltage-gated Ca^{2+} current (see Rieke & Schwartz, 1994). The phase angle was tuned to minimize the effect of changes in series conductance on the capacitance measurement. Analysis of the sine (in-phase) and cosine (out-of-phase) current components produced two traces: one was proportional to cell conductance; the other was proportional to the cell capacitance. Conductance and capacitance traces were calibrated by computer-controlled steps in the compensation circuit of the List EPC7 amplifier. A change in conductance compensation had little effect on the capacitance trace (Fig. 1*A*).

* To whom correspondence should be addressed.

Results were rejected if the conductance changed more than 0·1 nS after the calibration pulses.

Two observations indicated that a capacitance change occurred only in the synaptic terminal and required a change in Ca^{2+} concentration. First, photolysis of DM-nitrophen did not produce a capacitance change in rods whose synaptic terminal was amputated during the dissociation procedure (Fig. 1*B*; 8 cells). Second, photolysis of caged acetic acid, a compound that should not alter the intracellular Ca^{2+} concentration, did not produce a capacitance change in cells with intact synaptic terminals (5 cells).

Fluo-3 was excited with 480 ± 20 nm light from a 75 W xenon arc lamp. Ca^{2+} buffers were photolysed with ultraviolet light (1·6 mW cm^{-2} between 340 and 400 nm in the object plane) from a 200 W mercury arc lamp. Shutters allowed independent control of the light from each source. Beams of light from each source were combined with a 400 nm dichroic filter and reflected into the microscope objective (Plan-NEOFLUAR ×40/0·85, Carl Zeiss, Germany). Images were recorded with a camera (model AT200; Photometrics, Tucson, AZ, USA) containing a Kodak 1400 CCD. Each pixel was 0·17 × 0·17 μm in the plane of focus. Two-dimensional imaging allowed us to recognize and eliminate experiments with a significant amount of light scatter or a change in cell shape. Light scattered from the soma or the recording pipette was measured in a region next to the terminal. Scattered light was insignificant as long as the terminal was located 5–6 μm from the soma. Changes in shape were observed by superimposing fluorescence images recorded at the beginning and end of each experiment. Results from cells that changed shape during an experiment were discarded.

Fluorescence images produced by minimum and maximum Ca^{2+} concentrations were measured at the end of each experiment. The minimum image was measured by puffing a solution containing 10 mM EGTA and no Ca^{2+} over the cell. Fluorescence reached a steady minimum in 60–120 s. Subsequent exposure to a Ca^{2+} ionophore (either 10 μM 4-bromo A-23187, 81 cells; or 10 μM ionomycin, 8 cells) did not further decrease the fluorescence. The maximum image was measured by maintaining a potential of −30 mV to open Ca^{2+} channels and puffing a solution containing 20 mM Ca^{2+} over the cell. Again the fluorescence was monitored until a steady maximum was reached. Exposure to a Ca^{2+} ionophore did not produce a further change in fluorescence. The number of photons in each pixel was converted to fractional fluorescence, f, using the corresponding pixel values from the minimum (i_{min}) and maximum (i_{max}) images,

$$f = (i - i_{min})/(i_{max} - i_{min}). \quad (1)$$

The ratio i_{max}/i_{min} was approximately 50 for fluo-3 in saline and 20–40 for fluo-3 in cells. The lower ratio measured in cells may be due to autofluorescence or a fraction of the dye partitioning into organelles. However, since these effects contribute equally to i, i_{min} and i_{max}, they should not cause systematic errors in Ca^{2+} measurement. If fluo-3 has a single Ca^{2+} binding site with a dissociation constant K_D, then the Ca^{2+} co

ncentration, $[Ca^{2+}]$, is:

$$[Ca^{2+}] = K_D f/(1 - f). \quad (2)$$

The relation between Ca^{2+} concentration and fractional fluorescence, f, was fitted by eqn (2) to determine the K_D. Calibration solutions (adjusted to pH 7·20 with NaOH and 220 mosmol kg^{-1} with NaCl)

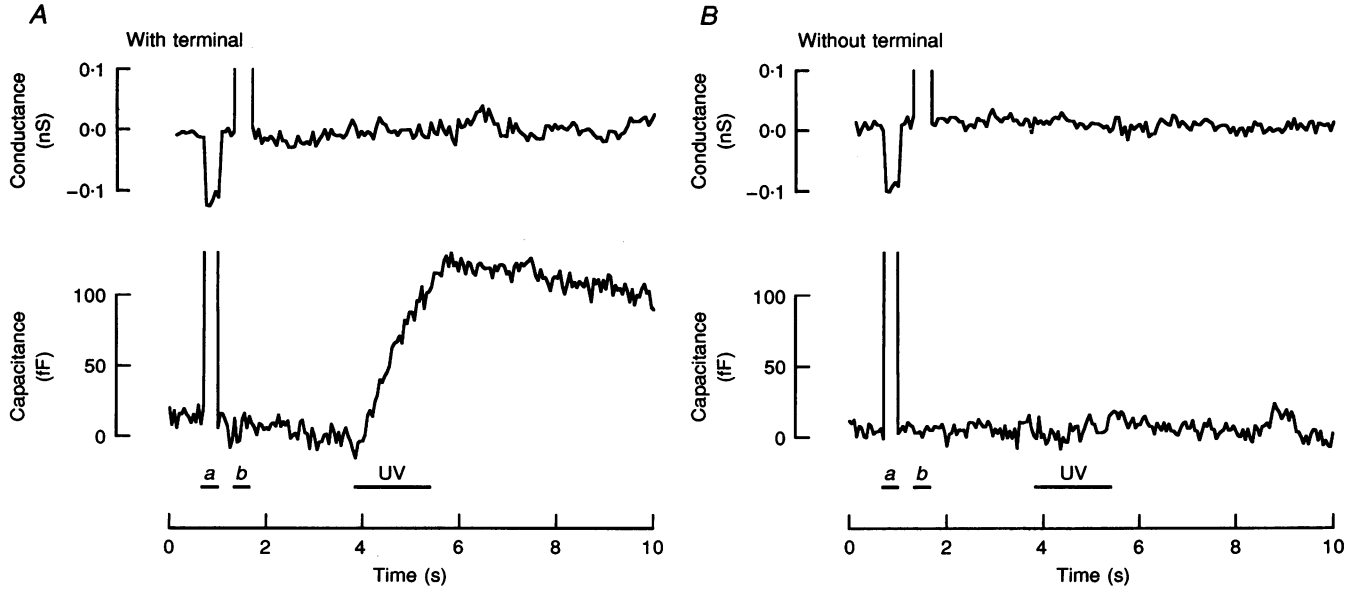

Figure 1. Calibration of the change in capacitance

Solitary rods were studied in the whole-cell, tight-seal configuration. The recording pipettes contained 3 mM DM-nitrophen, 2 mM Ca^{2+} and 0·1 mM fluo-3. Conductance (upper traces) and capacitance (lower traces) traces were calibrated by computer-controlled steps in the compensation circuit of the voltage clamp amplifier: first a 500 fF increase (horizontal bar labelled *a*) and then a 50 nS increase (horizontal bar labelled *b*). The calibrations are off scale, but can be measured when the traces are viewed at low gain. The high gain used in the figure demonstrates that a change in conductance (*b*) was not reflected in the capacitance trace. In addition, photolysis of a caged Ca^{2+} buffer (during the period indicated by the horizontal bar labelled UV) produced a capacitance increase only when a rod had an attached synaptic terminal (*A*) and failed to produce a capacitance change when the terminal was absent (*B*).

between 140 and 700 nM; 10 mM *N*-hydroxy-ethylethylene-diamine-triacetic acid (HEDTA) for Ca^{2+} concentrations between 1 and 10 μM; and 10 mM nitrilotriacetic acid (NTA) for Ca^{2+} concentrations between 25 and 100 μM. Ca^{2+} concentrations were checked with a Ca^{2+}-sensitive electrode (Microelectrodes Inc., Londonderry, NH, USA). The fractional fluorescence, f, is plotted against Ca^{2+} concentration in Fig. 2 (closed circles). The continuous curve is predicted by a Hill equation assuming a single Ca^{2+} binding site with a K_D of 0·4 μM.

The K_D of fluo-3 may decrease 2- to 3-fold in cytoplasm (Harkins, Kurebayashi & Baylor, 1993). The following procedure was used to estimate the K_D during whole-cell recording. Whole-cell, tight-seal recordings were established with pipettes containing 0·1 mM fluo-3 and 10 mM HEDTA adjusted to a free Ca^{2+} concentration of 1 μM. After allowing 5 min for the contents of the cytoplasm to exchange with the solution in the pipette, the fluorescence was measured. Next, the cell was superfused with saline solutions containing a Ca^{2+} ionophore and minimum and maximum images were recorded (as described above). The fractional fluorescence, f, calculated from the three measurements was 0·55 ± 0·03 (5 cells). We assumed that the stoichiometry between Ca^{2+} and fluo-3 was the same as in saline. Consequently, we could determine the K_D by drawing a Hill curve through this single point. The K_D determined by this method, 0·8 ± 0·1 μM, was used to rescale the fluorescence recorded from cells studied in the whole-cell, tight-seal configuration with pipettes that contained fluo-3 plus either nitr-5 or diazo-2 (Fig. 5*B* and *C*).

The K_D for perforated-patch recording was measured after intact cells were incubated in fluo-3 AM (as described above). Rods were superfused with a series of saline solutions containing a Ca^{2+} ionophore: the first saline solution contained a buffered Ca^{2+} concentration, the next contained 10 mM EGTA and no Ca^{2+}, and the last saline solution contained 2 mM Ca^{2+}. In each instance, the fluorescence was monitored until a stable level was reached. Measurements of f made on thirty-eight cells are plotted by the open circles in Fig. 2. The dashed line is predicted by a Hill equation with a dissociation constant of 1·0 μM. This value was used to calibrate fluorescence measurements made during perforated-patch recording (Figs 3 and 4).

The K_D values of fluo-3 in saline (0·4 μM), in cytoplasm during whole-cell recording (0·8 μM), and during permeabilized-patch recording (1·0 μM) indicate a systematic effect of intracellular viscosity and cytoplasmic proteins (see also Harkins *et al.* 1993).

Photolabile compounds can alter the apparent K_D of fluo-3. Therefore, the K_D was remeasured in the presence of 3 mM DM-nitrophen, 4 mM nitr-5 or 1 mM diazo-2. Calibration solutions were corrected for Ca^{2+} binding to the photolabile buffer (dissociation constants of 4 nM for DM-nitrophen, 140 nM for nitr-5, and 2 μM for diazo-2). Nitr-5 and diazo-2 did not affect the apparent K_D of fluo-3. However, DM-nitrophen, as reported by Zucker (1992), produced a large change and shifted the K_D to 1·5 μM. The value measured in saline was further altered by the cytoplasmic environment. The fractional fluorescence measured after cells exchanged with a pipette solution containing 0·1 mM fluo-3, 3 mM DM-nitrophen and 10 mM HEDTA, adjusted to a free Ca^{2+} concentration of 1 μM, was 0·30 ± 0·03 (5 cells). A Hill curve drawn through this point has a K_D of 2·3 ± 0·3 μM. This K_D value was used to rescale the fluorescence recorded from cells studied in the whole-cell, tight-seal configuration with intracellular fluo-3 plus DM-nitrophen (Fig. 5*A*).

Sources

Diazo-2, DM-nitrophen, nitr-5 and leupeptin were obtained from Calbiochem; 4-bromo A-23187, fluo-3 and caged acetic acid from Molecular Probes; $CaCl_2$ from BDH Laboratory Supplies; and amino acid and vitamin supplements were from Gibco. Nisoldipine was a gift from A. Fox (University of Chicago, USA). The SAL-1 antibody used to attach cells to glass coverslips was a gift from P. R. MacLeish (Cornell University Medical College, New York). All other chemicals were obtained from Sigma.

RESULTS

Steady-state, intraterminal Ca^{2+} concentration

We first measured the Ca^{2+} concentration in the synaptic terminal as membrane voltage was varied within the physiological range. Solitary rods were voltage clamped in the perforated-patch configuration while the intracellular Ca^{2+} concentration was measured with the dye fluo-3. Figure 3*A* shows a bright-field image of a rod inner segment, axon and synaptic terminal. Figure 3*B* and *C* show steady-state fluorescence images obtained at different holding potentials. As described in the Methods, the number of photons measured in each pixel has been rescaled to indicate the Ca^{2+} concentration. Ca^{2+} concentrations across a line of pixels (indicated by arrows at the left of Fig. 3*B*

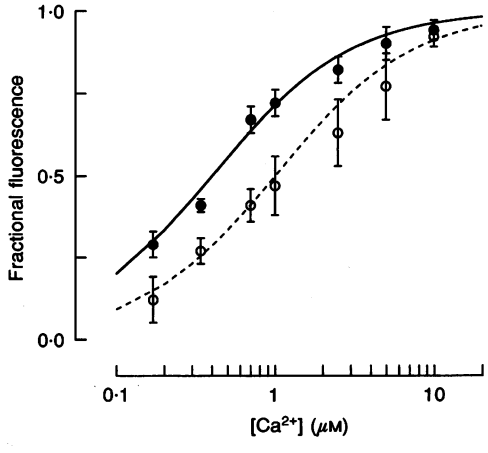

Figure 2. Calibration of fluo-3 fluorescence
Fractional fluorescence, f, is plotted as a function of Ca^{2+} concentration. The filled circles show measurements made for fluo-3 in saline. The continuous line through the data is predicted by a Hill equation for one binding site with a K_D of 0·4 μM. The open circles show measurements made from cells loaded with fluo-3 AM. Each point is the mean of measurements from 4–6 cells (total of 38 cells). The dashed line is predicted by a Hill equation for one binding site with a K_D of 1·0 μM. Vertical bars are ± 1 S.D. See Methods.

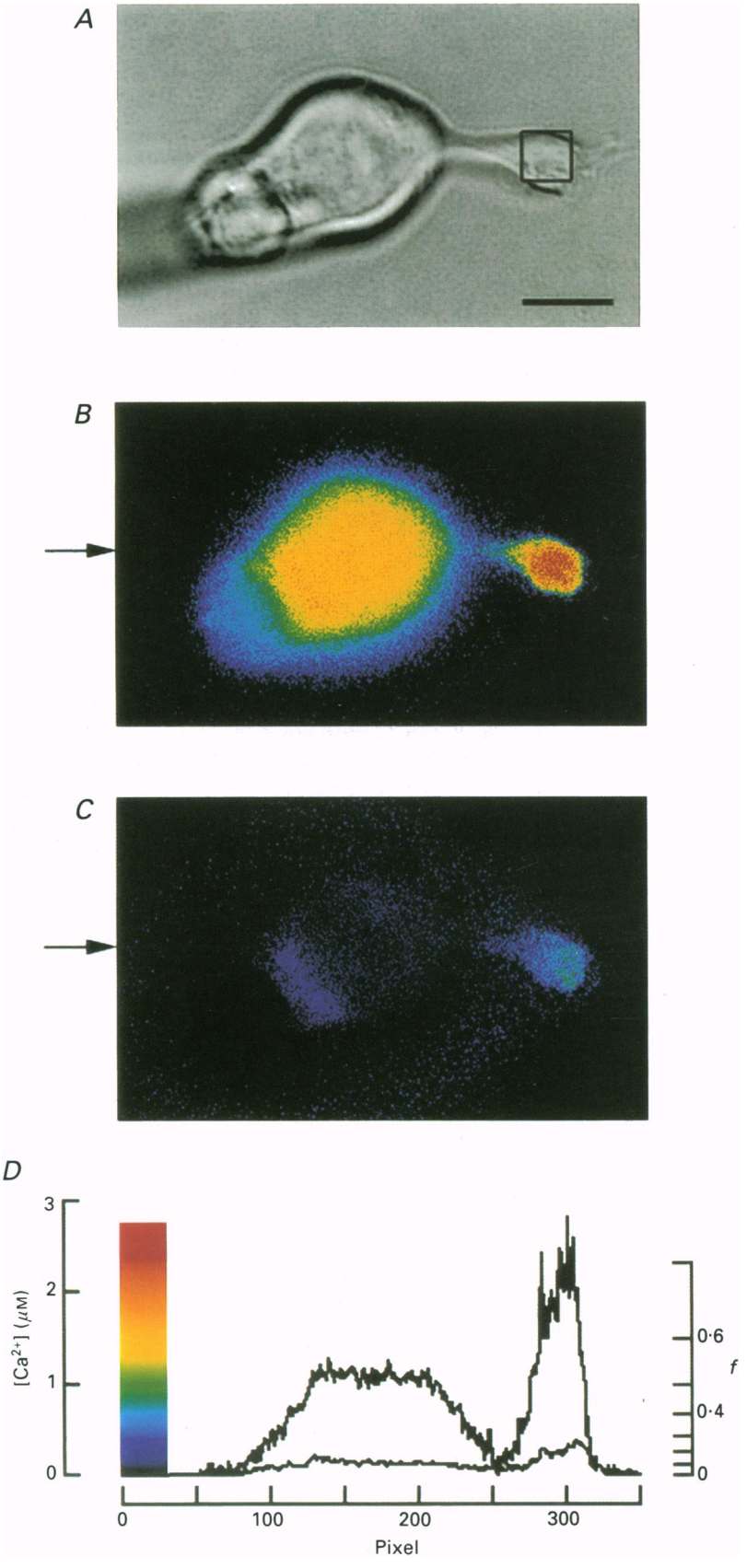

Figure 3. Imaging the Ca^{2+} concentration in a rod inner segment and synaptic terminal

A, bright-field image. A recording pipette attached in the perforated-patch configuration is visible at the left of the cell above the plane of focus. The square centred over the synaptic terminal is $5{\cdot}3 \times 5{\cdot}3\ \mu m^2$. The scale bar indicates 10 μm. *B*, fluorescence image acquired at −40 mV. Fluorescence counts were converted to Ca^{2+} concentration as described in the Methods using a K_D of 1 μM. The pseudocolour scale is shown adjacent to the left-hand axis in *D*. *C*, fluorescence image acquired at −50 mV. *D*, calcium profiles. Superimposed traces are the Ca^{2+} concentrations in the row of pixels indicated by arrows in *B*(−40 mV) and *C*(−50 mV). Fractional fluorescence, *f*, defined by eqn (1) is plotted on the right-hand axis. Ca^{2+} concentration calculated from eqn (2) is plotted on the left-hand axis.

and C) are plotted in Fig. 3*D*. Fluorescence counts in a 5·3 μm^2 region (outlined square in Fig. 3*A*) were summed and rescaled to obtain the spatially averaged Ca^{2+} concentration in the terminal. For the cell in Fig. 3, the average Ca^{2+} concentration in the terminal was 2·2 μM at −40 mV (Fig. 3*B*) and 0·2 μM at −50 mV (Fig. 3*C*).

The steady-state Ca^{2+} concentration measured in eight rod synaptic terminals is plotted in Fig. 4. The Ca^{2+} concentration changed little as rods were depolarized from −55 to −45 mV and then increased e-fold with each 4 mV additional depolarization (dashed line in Fig. 4). The voltage dependence of the Ca^{2+} concentration is similar to the voltage dependence of the whole-cell Ca^{2+} current, which increases e-fold for each 4·5 mV depolarization between −45 and −35 mV (see Rieke & Schwartz, 1994, and references therein). When voltage-activated Ca^{2+} channels were blocked with 5 μM nisoldipine, the cytoplasmic Ca^{2+} concentration in the terminal was unaffected by shifting the voltage between −60 and −20 mV (5 cells, data not shown). Thus, voltage appears to modulate Ca^{2+} entry into the rod synaptic terminal solely by controlling the opening of voltage-activated Ca^{2+} channels.

Exocytosis and endocytosis

The opening of a Ca^{2+} channel produces a rapid, local change in Ca^{2+} concentration that is difficult to detect with an imaging system (see Llinás, Sugimori & Silver, 1992). To avoid these evanescent changes in Ca^{2+} concentration, we changed the Ca^{2+} concentration throughout the cytoplasm by photolysis of a photolabile Ca^{2+} buffer. Consistent results were obtained with two photolabile buffers which raised the Ca^{2+} concentration and one photolabile buffer which lowered the Ca^{2+} concentration (see below).

Vesicle cycling produces changes in cell surface area that can be measured as changes in membrane capacitance (Neher & Marty, 1982; Kado, 1993); capacitance increases when the rate of exocytosis exceeds the rate of endocytosis and decreases when endocytosis exceeds exocytosis. We recorded in the whole-cell configuration and exchanged the cytoplasm with a pipette solution containing Ca^{2+}–DM-nitrophen (Kaplan & Ellis-Davis, 1988). Membrane capacitance was measured with a digital phase-sensitive detector (see Methods). We used an ultraviolet light source to photolyse DM-nitrophen and a second light source to measure fluo-3 fluorescence. We adjusted the intensity and duration of the ultraviolet light so that the time course of Ca^{2+} change resembled the voltage response normally produced when a rod absorbs visible light. Photolysis produced parallel increases in Ca^{2+} concentration (Fig. 5*A*, thin trace) and capacitance (thick trace). After photolysis, both traces slowly returned to their original levels. Complete recovery required a few minutes, a time sufficient for the exchange of photolysed buffer in the cell with unphotolysed buffer in the recording pipette. The similar shape of the two traces demonstrates that the capacitance change was approximately proportional to the Ca^{2+} concentration. The proportionality factor between Ca^{2+} concentration and capacitance can be estimated by matching the amplitudes of the two traces (i.e. β is the factor of proportionality between the left and right ordinates in Fig. 5*A*). In eight cells β was 48 ± 28 fF μM^{-1} (mean ± S.D.).

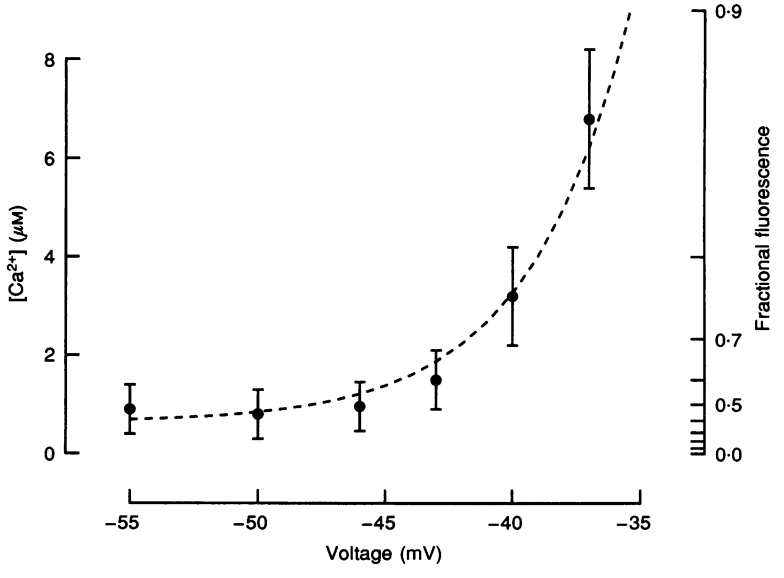

Figure 4. Voltage dependence of the steady-state Ca^{2+} concentration

The holding potential was first maintained at −37 mV and then hyperpolarized in a series of 30 s steps to −55 mV. At each holding potential, the Ca^{2+} concentration in the synaptic terminal (see Fig. 3) was measured as described in the Methods using a K_D of 1·0 μM. Data from 8 rods; means ± S.D. The dashed line is $[Ca^{2+}] = C_0 \exp(V/B) + C_1$, where V is voltage and B, C_0 and C_1 are constants (B = 4 mV, C_0 = 62 mM and C_1 = 0·5 μM).

Photolysis decreases the affinity constant of DM-nitrophen from 4 nM to approximately 2 mM and, in our experiments, raised the free Ca^{2+} concentration to 5–10 μM, a level higher than that maintained in rod terminals under physiological conditions (see Fig. 4). A more modest change in Ca^{2+} concentration can be insured by using nitr-5 (Adams, Kao, Gryniewicz, Minta & Tsien, 1988), a buffer whose affinity for Ca^{2+} decreases during photolysis from 140 nM to 6 μM. In the example illustrated in Fig. 5*B*, photolysis of nitr-5 raised the Ca^{2+} concentration from 0·4 to 2 μM and increased the capacitance by 60 fF. Uniformly raising the Ca^{2+} concentration to 2 μM, a value slightly less than the spatially averaged concentration at −40 mV (see Fig. 4), was sufficient to produce a capacitance increase.

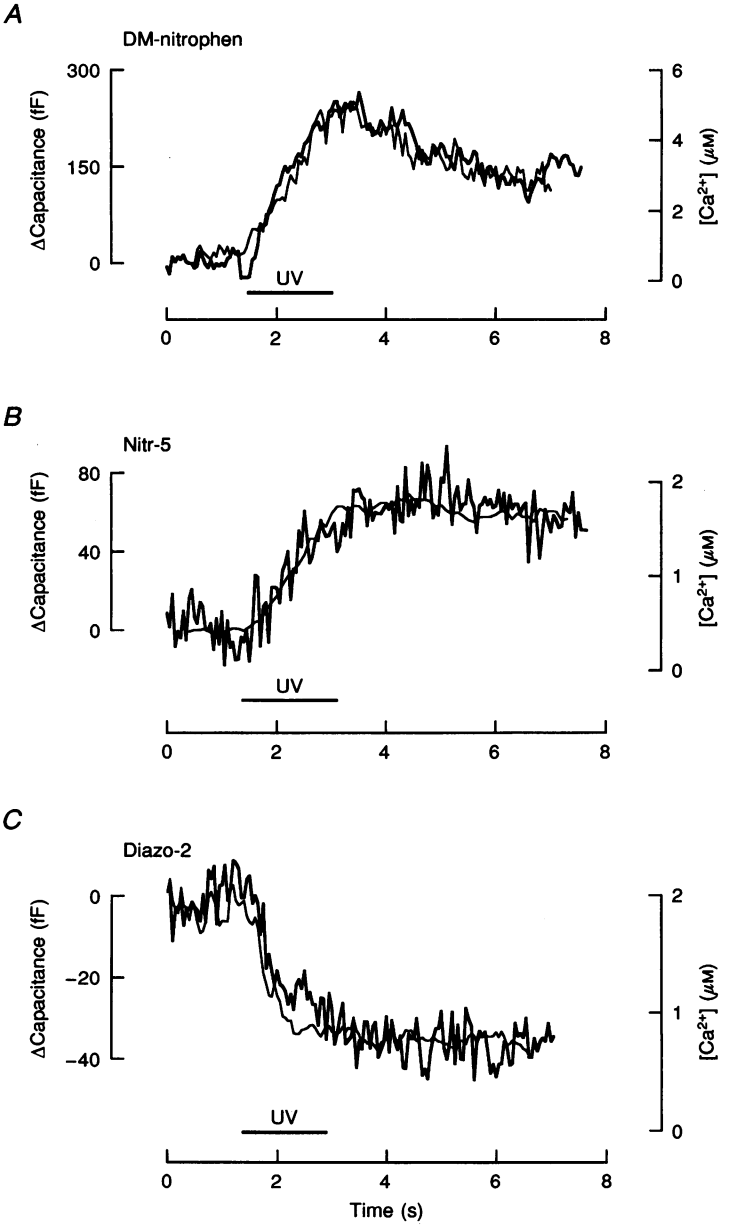

Figure 5. Capacitance change produced by a physiological change in average cytoplasmic Ca^{2+} concentration

Solitary rods were studied in the whole-cell, tight-seal configuration. Thick trace, change in capacitance; thin trace, change in cytoplasmic Ca^{2+} concentration. Cells were irradiated with ultraviolet light during the period indicated by the horizontal bars labelled UV. *A*, DM-nitrophen. The recording pipette contained 3 mM DM-nitrophen, 2 mM Ca^{2+} and 0·1 mM fluo-3. *B*, nitr-5. The recording pipette contained 4 mM nitr-5, 2 mM Ca^{2+} and 0·1 mM fluo-3. *C*, diazo-2. The recording pipette contained 1 mM diazo-2, 0·5 mM Ca^{2+} and 0·1 mM fluo-3. Fluorescence counts measured in the synaptic ending were converted to Ca^{2+} concentration as described in Methods using a K_D of 2·3 μM in *A* and 0·8 μM in *B* and *C*.

The time courses of the increase in Ca^{2+} concentration and capacitance were similar; the proportionality factor, β, between Ca^{2+} concentration and capacitance was 42 ± 23 fF μM^{-1} (6 cells; mean ± S.D.).

Complementary experiments were completed with diazo-2 (Adams, Kao & Tsien, 1989), a Ca^{2+} buffer that changes its K_D from 2·2 μM to 70 nM upon photolysis. In the experiment illustrated in Fig. 5*C*, ultraviolet illumination decreased the free Ca^{2+} concentration from 2 to 0·7 μM and decreased the capacitance by 35 fF. Again the traces have similar shapes and can be scaled with a proportionality factor, β, equal to 30 ± 16 fF μM^{-1} (7 cells; mean ± S.D.).

The diazo-2 experiments emulate the normal physiological function of rod photoreceptors. During darkness a rod maintains a potential of −40 mV and a steady Ca^{2+} concentration of 2–4 μM. Absorption of light in the outer segment hyperpolarizes the cell, closes voltage-gated Ca^{2+} channels, and reduces the Ca^{2+} concentration in the terminal. Photolysis of diazo-2 produced a similar Ca^{2+} concentration change. Prior to photolysis, the capacitance was constant, indicating that the rates of exocytosis and endocytosis were balanced in a steady state. During photolysis, the Ca^{2+} concentration declined and the balance was upset. The decrease in capacitance indicates that the rate of endocytosis briefly exceeded the rate of exocytosis. Subsequently, when a new steady state was achieved after 1–2 s, the capacitance was again constant and the rates of exocytosis and endocytosis were again equal. How quickly did a change in endocytosis follow exocytosis? The decline in capacitance can be described by a time constant of 0·7 s. If exocytosis stopped the moment photolysis commenced, then the decline in capacitance would be determined only by endocytosis. Alternatively, if the decline in the rate of exocytosis was proportional to the Ca^{2+} concentration, then the lag between exocytosis and endocytosis would be less. A similar conclusion can be reached from experiments with DM-nitrophen (Fig. 5*A*). A lag between exocytosis and endocytosis would cause the capacitance trace to reach a peak after the Ca^{2+} concentration. The disparity in the times to peak of the Ca^{2+} concentration and capacitance traces was always less than 0·5 s (8 cells). Thus, endocytosis followed exocytosis with a lag that was probably less than 0·5 s and certainly less than 0·7 s.

The diazo-2 experiments allow us to calculate a lower bound for the rate of vesicle fusion during physiological function. Changing the Ca^{2+} concentration from 2 to 0·7 μM decreased the capacitance by approximately 35 fF in 1 s (Fig. 5*C*). If each 45 nm vesicle contributed 0·08 fF, the change in capacitance is equivalent to the retrieval of 400 vesicles in 1 s. Since exocytosis and endocytosis were balanced in the steady state that preceded photolysis, the rate of exocytosis at 2 μM Ca^{2+} must be greater than 400 vesicles s^{-1}. Even though we were unable to measure exocytosis and endocytosis separately, it is apparent that both processes must normally proceed at a prodigious rate.

DISCUSSION

'Pulse' synapses made by spiking cells operate with a characteristic fast response time. A short delay, e.g. less than 200 μs at the squid giant synapse (Llinás, Steinberg & Walton, 1981), leaves little time for diffusion and indicates that Ca^{2+} channels and fusion sites must be close together. The following picture has emerged (reviewed by Augustine *et al.* 1987). The average Ca^{2+} concentration in the cytoplasm is low, perhaps only 100 nM. Depolarization opens Ca^{2+} channels and causes a rapid, local increase in Ca^{2+} concentration. Exocytosis requires the simultaneous action of several Ca^{2+} ions and is half-activated by 100–200 μM Ca^{2+}. As a result, fusion occurs only at sites that are immediately adjacent to an open Ca^{2+} channel.

'Graded' synapses in rods operate differently. Their task is to transmit the small and slow voltage change produced by the absorption of a single photon. The opening of each Ca^{2+} channel produces a brief Ca^{2+} influx which dissipates through diffusion and contributes to the average cytoplasmic Ca^{2+} concentration. The spatially averaged Ca^{2+} concentration at −40 mV is 2–4 μM (Fig. 4), sufficient to sustain a high rate of vesicle cycling (Fig. 5*B* and *C*). Vesicle fusion sustained by the average Ca^{2+} concentration is not coordinated with the opening of individual Ca^{2+} channels. Of course, asynchronous fusion may be supplemented by synchronous fusion if microdomains overlap fusion sites. Controlling transmitter release with the average Ca^{2+} concentration will decrease temporal resolution. However, resolution on a millisecond scale is unimportant for transmitting single photon responses that take 0·5–1 s to reach peak. The temporal filtering produced by diffusion and buffering may improve the signal-to-noise characteristics of small, slow presynaptic signals.

Different cells in the retina have synapses with quite different functional characteristics. Bipolar cells act as contrast detecting flip-flops, relaying graded information to the inner synaptic layer where transient responses develop. Exocytosis in bipolar cells requires Ca^{2+} concentrations above 10–20 μM (Heidelberger, Heinemann, Neher & Matthews, 1994). Endocytosis lags exocytosis with a time constant of several seconds and stops when the Ca^{2+} concentration is greater than 1 μM (von Gersdorff & Matthews, 1994). Consequently, neither process should operate when the average Ca^{2+} concentration is maintained between 1 and 10 μM. In contrast, rods transmit graded signals produced by the absorption of a few photons. Exocytosis and endocytosis are balanced at steady physiological Ca^{2+} concentrations greater than 1–2 μM. Exocytosis and endocytosis must be precisely coordinated; even a slight imbalance would be catastrophic for a cell that can remain depolarized and sustain continuous fusion for many hours. Changes in exocytosis are balanced by endocytosis in less than 0·7 s. The graded synapse used by rods and the pulse synapse used by bipolar cells may represent two extremes of synaptic function.

Other synapses may combine graded and pulse behaviour. The neuromuscular junction (Barrett & Stevens, 1972), synapses between hippocampal neurons in culture (Goda & Stevens, 1994) and synapses between retinal amacrine cells in culture (Gleason, Borges & Wilson, 1994) have two mechanistic components for vesicle fusion. One component has a low Ca^{2+} affinity and synchronously couples Ca^{2+} channel opening with vesicle fusion; the other component has a higher Ca^{2+} affinity and asynchronously couples channel opening and fusion. The relative contributions of the two mechanisms may be altered at different synapses to optimally transmit presynaptic signals.

Adams, S. R., Kao, J. P. Y., Gryniewicz, G., Minta, A. & Tsien, R. Y. (1988). Biologically useful chelators that release Ca^{2+} upon illumination. *Journal of the American Chemical Society* **110**, 3212–3220.

Adams, S. R., Kao, J. P. Y. & Tsien, R. Y. (1989). Biologically useful chelators that take up Ca^{2+} upon illumination. *Journal of the American Chemical Society* **111**, 7957–7968.

Augustine, G. J., Charlton, M. P. & Smith, S. J. (1987). Calcium action in synaptic transmitter release. *Annual Review of Neuroscience* **10**, 633–693.

Barrett, E. F. & Stevens, C. F. (1972). The kinetics of transmitter release at the frog neuromuscular junction. *Journal of Physiology* **227**, 691–708.

Capovilla, M., Hare, W. A. & Owen, W. G. (1987). Voltage gain of signal transfer from retinal rods to bipolar cells in the tiger salamander. *Journal of Physiology* **391**, 125–140.

Gleason, E., Borges, S. & Wilson, M. (1994). Control of transmitter release from retinal amacrine cells by Ca^{2+} influx and efflux. *Neuron* **13**, 1109–1117.

Goda, Y. & Stevens, C. F. (1994). Two components of transmitter release at a central synapse. *Proceedings of the National Academy of Sciences of the USA* **91**, 12942–12946.

Harkins, A. B., Kurebayashi, N. & Baylor, S. M. (1993). Resting myoplasmic free calcium in frog skeletal muscle fibers estimated with fluo-3. *Biophysical Journal* **65**, 865–881.

Hecht, S., Shlaer, S. & Pirenne, M. H. (1942). Energy, quanta, and vision. *Journal of General Physiology* **25**, 819–840.

Heidelberger, R., Heinemann, C., Neher, E. & Matthews, G. (1994). Calcium dependence of the rate of exocytosis in a synaptic terminal. *Nature* **371**, 513–515.

Joshi, C. & Fernandez, J. M. (1988). Capacitance measurements. An analysis of the phase detector technique used to study exocytosis and endocytosis. *Biophysical Journal* **53**, 885–892.

Kado, R. T. (1993). Membrane area and electrical capacitance. *Methods in Enzymology* **221**, 273–299.

Kaplan, J. H. & Ellis-Davis, G. C. R. (1988). Photolabile chelators for the rapid photorelease of divalent cations. *Proceedings of the National Academy of Sciences of the USA* **85**, 6571–6575.

Llinás, R., Steinberg, I. Z. & Walton, K. (1981). Relationship between presynaptic calcium current and postsynaptic potential in squid giant synapse. *Biophysical Journal* **33**, 323–351.

Llinás, R., Sugimori, M. & Silver, R. B. (1992). Microdomains of high calcium concentration in a presynaptic terminal. *Science* **256**, 677–679.

Neher, E. & Marty, A. (1982). Discrete changes of cell membrane capacitance observed under conditions of enhanced secretion in bovine adrenal chromaffin cells. *Proceedings of the National Academy of Sciences of the USA* **79**, 6712–6716.

Rieke, F. & Schwartz, E. A. (1994). A cGMP-gated current can control exocytosis at cone synapses. *Neuron* **13**, 863–873.

Rieke, F. & Schwartz, E. A. (1995). Exocytosis and calcium homeostasis at a slow synapse. *Biophysical Journal* **68**, A14.

Schwartz, E. A. (1976). Electrical properties of the rod syncytium in the retina of the turtle. *Journal of Physiology* **257**, 379–406.

Trifonov, Yu. A. (1968). Study of synaptic transmission between the photoreceptor and the horizontal cell using electrical stimulation of the retina. *Biofizika* **13**, 809–817.

von Gersdorff, H. & Matthews, G. (1994). Inhibition of endocytosis by elevated internal calcium in a synaptic terminal. *Nature* **370**, 652–655.

Zucker, R. S. (1992). Effects of photolabile Ca chelators on fluorescent Ca indicators. *Cell Calcium* **13**, 29–40.

Acknowledgements

Support was provided by the National Institutes of Health through grants R37-EY02440 to E.A.S. and F32-EY06456 to F.R. and a Research to Prevent Blindness Senior Investigator Award to E.A.S.

Author's present address

F. Rieke: Department of Neurobiology, Fairchild D-238, Stanford University, Stanford, CA 94305, USA.

Author's email address

E. A. Schwartz: eas@hearts.bsd.uchicago.edu

Received 31 August 1995; accepted 18 December 1995.